Inorg. Chem. **2008**, *47*, 1295−1300

Electrochemical Synthesis, Structural Characterization, and Decomposition of Rhenium Oxoethoxide, $Re_4O_4(OEt)_{12}$. Ligand Influence on the Structure and Bonding in the High-Valent Tetranuclear Planar Rhenium Alkoxide Clusters

Olesya A. Nikonova,[†,‡] Kjell Jansson,[§] Vadim G. Kessler,[†] Margareta Sundberg,[§] Alexei I. Baranov,[⊥,△] Andrei V. Shevelkov,[⊥] Dmitrii V. Drobot,[‡] and Gulaim A. Seisenbaeva*[,†]

Department of Chemistry, SLU, Box 7015, SE-750 07 Uppsala, Sweden, Moscow State Academy of Fine Chemical Technology, Pr. Vernadskogo 86, 117571 Moscow, Russia, Inorganic Chemistry, Arrhenius Laboratory, Stockholm University, SE-106 91 Stockholm, Sweden, Department of Chemistry, Moscow State University, 119991 Moscow, Russia, and Max-Plank Institute for Chemical Physics of Solids, 01187-Dresden, Germany

Received September 11, 2007

Anodic oxidation of rhenium in ethanol in the presence of LiCl as a conductive additive results with high yield in formation of a new oxoethoxide cluster, $Re_4O_4(OEt)_{12}$. The structure of the planar centrosymmetric metal–oxygen core of this molecule is composed of four edge-sharing $Re(V)O_6$ octahedra. Eight electrons are available for the formation of metal−metal bonds indicated by five relatively short Re−Re distances within the Re_4-rhombus, a "planar butterfly" type cluster. The theoretical calculations are indicating relatively low contribution of metal−metal bonding in the stability of the core. The stability of the +V-oxidation state, unusual for rhenium alkoxides can be at least partially attributed to the size effects in the packing of ligands. The X-ray powder study indicates that treatment of $Re_4O_4(OEt)_{12}$ in ambient atmosphere rapidly transforms it into a mixed-valence derivative $Re_4O_6(OEt)_{10}$—with a structure related to the earlier investigated cluster $Re_4O_6(O^iPr)_{10}$. Thermal decomposition of the latter rhenium oxoethoxide results in reduction to rhenium metal at as low temperatures as 380 °C, producing aggregates of metal nanoparticles with the average size of 3 nm.

Introduction

The interest in rhenium alkoxides, derivatives of higher oxidation states V, VI, and VII, is caused by the possibility of their application as precursors for the preparation of highly reactive fine powders of rhenium metal or its alloys for powder metallurgy applications.[1,2] Recently demonstrated applications of rhenium oxides as selective catalysts in many oxidation reactions in organic synthesis have made the alkoxide derivatives also attractive for the synthesis of rhenium-based oxide nanocomposites.[3–5] An especially attractive application of rhenium complexes involving an alkoxide ligand lies in their activity in catalysis of metathesis reactions.[6] Formation of surface alkoxide can provide catalytic activity to the surface oxide species, offering heterogeneous metathesis catalysts.

The majority of synthetic approaches to rhenium alkoxides described in the literature are based either on the metathesis reactions of rhenium halides or oxide halides with alkoxides of other elements, most often alkali metals,[7] which brought about the isolation of $Re_2O_3(OMe)_6$, $Li_2Re_2O_2(O^iPr)_{10}$, and

* To whom correspondence should be addressed. E-mail: gulaim.seisenbaeva@kemi.slu.se.
† SLU.
‡ Moscow State Academy of Fine Chemical Technology.
§ Stockholm University.
⊥ Moscow State University.
△ Max-Plank Institute for Chemical Physics of Solids.

(1) Brookes, K. J. A. *Met. Powder Rep.* **2001**, *56*, 22.
(2) Leonhardt, T.; Trybus, C.; Hickman, R. *Powder Metall.* **2003**, *46*, 148.
(3) Topka, P.; Balcar, H.; Rathousky, J.; Zilkova, N.; Verpoort, F.; Cejka, J. *Microporous Mesoporous Mater.* **2006**, *96*, 44.
(4) Li, C. R.; Feng, Y. S.; Yang, Q. H. *Prog. Chem.* **2006**, *18*, 1482.
(5) Lacheen, H. S.; Cordeiro, P. J.; Iglesia, E. *J. Am. Chem. Soc.* **2006**, *128*, 15082.
(6) Schrock, R. R. *Polyhedron* **1995**, *14*, 3177.
(7) Edwards, P. G.; Wilkinson, G.; Hursthouse, M. B.; Malik, K. M. A. *J. Chem. Soc., Dalton Trans.* **1980**, 2467.

10.1021/ic701781k CCC: $40.75
Published on Web 01/26/2008

$ReO(O^tBu)_4$, or on interaction of rhenium heptoxide with alcohols (most often diols or polyols),[8,9] which led to isolation of $ReO_3(OR)$, R = Me, ^{t}Bu, $SiMe_3$, and $ReO(O_2R')_2$, R′ = C_6H_{12}, $C_{12}H_{20}$. These techniques are complicated by numerous side reactions, such as formation of stable alkoxide halide intermediates in metathesis reactions, for example, mixtures of $ReF_{6-x}(OMe)_x$ in co-condensation of ReF_6 with $Si(OMe)_4$[10] or by formation of the products of uncontrolled reduction in the reactions of Re_2O_7.[9]

We have shown earlier that the anodic oxidation of rhenium metal in alcohols is a facile and productive approach to the alkoxide derivatives of rhenium.[11–14] The process was investigated in such solvents as methanol and isopropanol, and it was found out that the reaction products in both cases were tetranuclear oxoalkoxide compounds, $Re_4O_{6-x}(OMe)_{12+x}$, containing mainly Re(VI)[11] and $Re_4O_6(O^iPr)_{10}$, where two atoms of Re(V) and two of Re(VI) were present in the same molecule.[12] The decomposition of both of these compounds in an inert atmosphere resulted in both cases in selective formation of ReO_3 at the temperatures of about 400 °C with subsequent reduction to ReO_2 by residual carbon at temperatures over 600 °C. The data on synthesis and thermal decomposition of the abovementioned rhenium alkoxides has recently been summarized in.[14]

It appeared interesting to study the oxidation of rhenium metal in ethanol and determine the factors supporting formation of derivatives of distinct oxidation states in both the electrochemical synthesis and the thermal decomposition in the thus completed homologous series.

Experimental Details

Handling of the samples and all procedures connected with the synthesis were carried out in inert (nitrogen or argon) atmosphere in a dry box. Dry ethanol (less than 0.02% H_2O, cat no. 100990) was purchased from Merck and used without further purification. LiCl for electrochemical experiments has been dried in air at 120−150 °C for at least 4 h and then in dynamic vacuum ($P \sim 1.3$ Pa) at 180–200 °C for 1 h. The dried LiCl samples were sealed in ampoules that were opened before each synthesis for the preparation of the electrolyte in a dry box.

IR spectra of nujol mulls were registered with a Perkin-Elmer FT-IR spectrometer Spectrum-100. Mass spectra were recorded using a JEOL JMS-SX/SX-102A mass spectrometer applying electron beam ionization ($U = 70$ eV) with direct probe introduction. The decomposition and sublimation processes in vacuum were studied in glass vessels evacuated by oil pump ($p = 10^{-2}$ mm m.c.). The gaseous products of decomposition were collected in the trap cooled with liquid nitrogen. After the decomposition process, the system was filled with dry nitrogen, and after warming to room temperature, a sample of the gas phase from the trap was investigated by GC-MS using a Hewlett-Packard 5890 Series II gas chromatograph supplied with a capillary separating column with a DB-Wax film phase (manufactured by J&W Scientific, CA) and coupled with a JEOL JMS-SX/SX102A Tandem mass spectrometer.

X-ray powder patterns of the samples were registered with a Guinier−Hägg camera using monochromatized Cu Kα radiation and silicon as an internal standard and with a STADI-P (STOE) diffractometer. Transmission electron micrographs and electron diffraction (ED) patterns of the samples were obtained in a JEOL 2000FX-II transmission electron microscope (TEM), equipped with a Link AN-10000 energy dispersive spectrometer (EDS) for microanalysis studies.

Thermogravimetric (TG) studies were carried out with a Perkin-Elmer TGA-7 device, and the measurements were performed in argon and nitrogen atmospheres, while the DSC thermograms were recorded with a Perkin-Elmer DSC-2 apparatus. The DSC equipment was calibrated both on temperature scale and enthalpy by use of metallic tin.

Theoretical analysis of bonding in $Re_4O_4(OEt)_{12}$ was carried out on the basis of molecular orbital diagrams calculated at the extended Hückel theory (EHT) level with the use of the CACAO[15] program package, applying a model with CH_3 groups as simplified analogs of the Et and ^{i}Pr ones for orbital diagram calculations.

Synthesis. Anodic dissolution of rhenium metal was carried out in a cell without subdivision into cathodic and anodic space, supplied with a reflux condenser and water cooling. LiCl was added to the concentration of about 0.025 M as an electrolyte. A platinum plate with the surface of 3.5 cm^2 was used as the cathode. A rhenium rod, 5 mm in diameter (Alfa Aesar cat. no. 00270), was used as the anode. The solution temperature was kept at ∼20−45 °C, voltage 170 V, total current 0.01–0.08 A, current density 0.04–0.05 A/cm^2, process duration 24 h. The electrolysis was associated with color changes from colorless to yellow and finally to reddish brown. Crystallization of dark brown plates was observed already during the process of electrochemical synthesis. The crystals were separated by decantation at the end of the process, washed with dry ethanol, and dried in vacuum, which offers rather dark, almost black samples. Yield was 70–90% with respect to the rhenium metal dissolved. The nature of the obtained product as $Re_4O_4(OEt)_{12}$ was established by repeated single crystal X-ray studies of randomly chosen samples. The elementary microanalysis data obtained by combustion techniques and involving quick transfer of the samples in air into the analyzer indicated slightly decreased content of carbon and hydrogen. Found, wt %: C 20.25; H 3.9. Calculated for $C_{24}H_{60}O_{16}Re_4$, wt %: C 21.36; H 4.5. Calculated for $C_{20}H_{50}O_{16}Re_4$, wt %: C 18.58; H 3.9. IR, cm^{-1}: 1303 w, 1167 w, 1154 w, 1082 w, 1005 w, 979 w, 906 s, 869 sh, 461 m (see also Figure FS1 in the Supporting Information).

Crystallography. The single crystal X-ray data (7090 independent reflections [R(int) = 0.0492]) were collected for $Re_4O_4(OEt)_{12}$ at low temperature (−120 °C) using an Xcalibur-3 Kappa-diffractometer (Oxford Diffraction Ltd.) (Mo Kα radiation, graphite monochromator). Triclinic, $P\bar{1}$, $a = 8.3591(7)$, $b = 10.4825(10)$, $c = 11.8092(19)$ Å, $\alpha = 72.742(11)$, $\beta = 72.282(11)$, $\gamma = 80.431(7)°$, $V = 938$ Å^3, $Z = 1$. The structure was solved by direct methods, and the coordinates of rhenium atoms were located from the initial solution. The coordinates of all other non-hydrogen atoms were located in subsequent difference Fourier syntheses. All non-hydrogen atoms were refined by full-matrix techniques first in

(8) Edwards, P. G.; Jokela, J.; Lehtonen, A.; Sillanpää, R. *Dalton Trans.* **1998**, 3287.
(9) Edwards, P. G.; Wilkinson, G. *J. Chem. Soc., Dalton Trans.* **1984**, 2695.
(10) Bryan, J. C.; Wheeler, D. R.; Clark, D. L.; Huffman, J. C.; Sattelberger, A. P. *J. Am. Chem. Soc.* **1991**, *113*, 3184.
(11) Seisenbaeva, G. A.; Shevelkov, A. V.; Kloo, L.; Gohil, S.; Tegenfeldt, J.; Kessler, V. G. *Dalton Trans.* **2001**, 2762.
(12) Shcheglov, P. A.; Seisenbaeva, G. A.; Drobot, D. V.; Kessler, V. G. *Inorg. Chem. Commun.* **2001**, *4*, 227.
(13) Kessler, V. G.; Shevelkov, A. V.; Kvorykh, G. V.; Seisenbaeva, G. A.; Turova, N. Ya.; Drobot, D. V. *Russ. J. Inorg. Chem.* **1995**, *40*, 1477.
(14) Shcheglov, P. A.; Drobot, D. V. *Russ. Chem. Bull., Int. Ed.* **2005**, *54*, 2247.
(15) Mealli, C.; Proserpio, D. M. *J. Chem. Educ.* **1990**, *67*, 3399.

Table 1. Selected Bond Distances (Å) and Angles (deg) in the Structure of the Low Temperature Phase of $Re_4O_4(OEt)_{12}$[a]

Re(1)−O(8)	1.872(4)	Re(2)−O(7)	1.951(4)
Re(1)−O(1)	1.877(4)	Re(2)−O(1)	1.993(4)
Re(1)−O(5)	1.946(4)	Re(2)−O(3)	2.031(5)
Re(1)−O(6)	2.077(4)	Re(2)−O(2)	2.046(4)
Re(1)−O(2)#1	2.065(4)	Re(2)−O(3)#1	2.053(4)
Re(1)−O(3)	2.072(4)	Re(2)−O(4)	2.055(5)
Re(1)−Re(2)	2.5358(5)	Re(2)−Re(2)#1	2.5511(5)
Re(1)−Re(2)#1	2.6301(6)	Re(2)−Re(1)#1	2.6301(6)
O(8)−Re(1)−O(1)	101.59(18)	O(7)−Re(2)−O(1)	89.03(17)
O(8)−Re(1)−O(5)	87.19(18)	O(7)−Re(2)−O(3)	87.21(18)
O(1)−Re(1)−O(5)	87.26(18)	O(1)−Re(2)−O(3)	99.46(17)
O(8)−Re(1)−O(6)	86.00(18)	O(7)−Re(2)−O(2)	84.90(17)
O(1)−Re(1)−O(6)	170.52(16)	O(1)−Re(2)−O(2)	171.42(17)
O(5)−Re(1)−O(6)	87.46(18)	O(3)−Re(2)−O(2)	86.32(18)
O(8)−Re(1)−O(2)#1	163.17(19)	O(7)−Re(2)−O(3)#1	169.01(19)
O(1)−Re(1)−O(2)#1	92.64(18)	O(1)−Re(2)−O(3)#1	84.66(16)
O(5)−Re(1)−O(2)#1	84.54(16)	O(3)−Re(2)−O(3)#1	102.68(15)
O(6)−Re(1)−O(2)#1	79.03(17)	O(2)−Re(2)−O(3)#1	100.34(16)
O(8)−Re(1)−O(3)	86.82(17)	O(7)−Re(2)−O(4)	87.15(18)
O(1)−Re(1)−O(3)	101.95(17)	O(1)−Re(2)−O(4)	88.30(17)
O(5)−Re(1)−O(3)	169.86(18)	O(3)−Re(2)−O(4)	170.33(16)
O(6)−Re(1)−O(3)	83.98(17)	O(2)−Re(2)−O(4)	85.36(18)
O(2)#1−Re(1)−O(3)	99.09(16)	O(3)#1−Re(2)−O(4)	83.68(17)
Re(1)−Re(2)−Re(1)#1	120.848(14)	Re(2)#1−Re(2)−Re(1)#1	58.582(14)

[a] Symmetry transformations used to generate equivalent atoms: #1 $-x, -y + 2, -z$.

isotropic and then anisotropic approximation. The coordinates of the hydrogen atoms were obtained by geometrical calculations and included into final refinement in isotropic approximation using riding model. The selected bond distances and angles are presented in Table 1. Final discrepancies were $R1 = 0.0377$, $wR2 = 0.0792$ [$I > 2\sigma(I)$]. All calculations have been carried out on an IBM PC using the SHELXTL-NT program package.[16]

The unit cell parameter determination has been carried out for the samples of $Re_4O_4(OEt)_{12}$ (sealed in an inert atmosphere) also at room temperature for identification purposes, giving triclinic, $P\bar{1}$, $a = 8.79(11)$, $b = 10.78$ (10), $c = 11.78(4)$ Å, $\alpha = 71.6(5)$, $\beta = 73.1(8)$, $\gamma = 81.7(9)°$, $V = 1012$ Å^3, and $Z = 1$.

Results and Discussion

The general appearance of the process of electrochemical synthesis seems almost analogous for the oxidation of metal in all three alcohols, indicating dissolution of metal in the oxidation state VI+ with subsequent partial (as in $Re_4O_{6-x}(OMe)_{12+x}$[11] or $Re_4O_6(O^iPr)_{10}$[17]) or complete reduction to Re(V) at the cathode. Formation of the final oxoalkoxide product occurs also with the high yields (70–90% in relation to the dissolved metal in the case of all the three alcohols). The reactions of electrochemical synthesis occur thus in an analogous way for all the three systems.

The nature of the solid crystalline products resulting from the processes is clearly different. In the case of the methoxide $Re_4O_{6-x}(OMe)_{12+x}$, the metal core is rectangular with two shorter Re(μ-OR)$_2$Re (3.455(3)–3.459(3) Å) and two longer Re−O−Re fragments (3.713(4)–3.740(6) Å). There are no metal−metal bonds in that structure based almost exclusively on Re(VI). The structure of the isopropoxide complex, $Re_4O_6(O^iPr)_{10}$, contains a planar rhombus of metal atoms with all five bonds of essentially the same length (2.52–2.55 Å,[17] compare Re═Re 2.532 Å in $Re_2(OMe)_{10}$[10]) which is rather short for the very low number of the electrons available for bonding

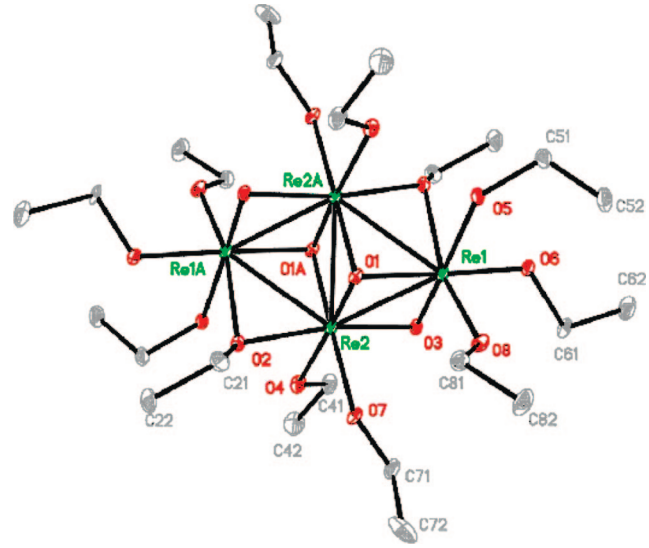

Figure 1. Molecular structure of $Re_4O_4(OEt)_{12}$.

in that structure (6 electrons for 5 bonds). The structure of $Re_4O_4(OEt)_{12}$ contains also a planar Re_4 core close to a rhombus in its geometry (see Figure 1 and Table 1). It belongs as well as the structure of the oxoisopropoxide derivative to the well-known M_4X_{16} core type structure type, originating from hexagonal dense packing of metal and ligand atoms, one of the most typical for metal alkoxides.[18,19] Two additional electrons available for bonding do not lead to pronounced shortening of the Re−Re distances; on the contrary, the structure of the compound $Re_4O_4(OEt)_{12}$ contains two shorter symmetrically equivalent bonds, and the shorter diagonals of the rhombus have almost the same lengths (2.5358(5) Å Re(1)−Re(2), 2.5511(5) Å Re2−Re2A), which is comparable with the length of a double Re═Re bond (see above).

(16) *SHELXTL-NT Reference Manual*; Bruker AXS: Madison, WI, 1998.
(17) Seisenbaeva, G. A.; Baranov, A. I.; Shcheglov, P. A.; Kessler, V. G. *Inorg. Chim. Acta* **2004**, *357*, 468.
(18) Wright, D. A.; Williams, D. A. *Acta Crystallogr.* **1968**, *24B*, 1107.
(19) Turova, N. Ya.; Turevskaya, E. P.; Kessler, V. G.; Yanovskaya, M. I. *The Chemistry of Metal Alkoxides*; Kluwer Academic Publishers: Boston, Dordrecht, London, 2002.

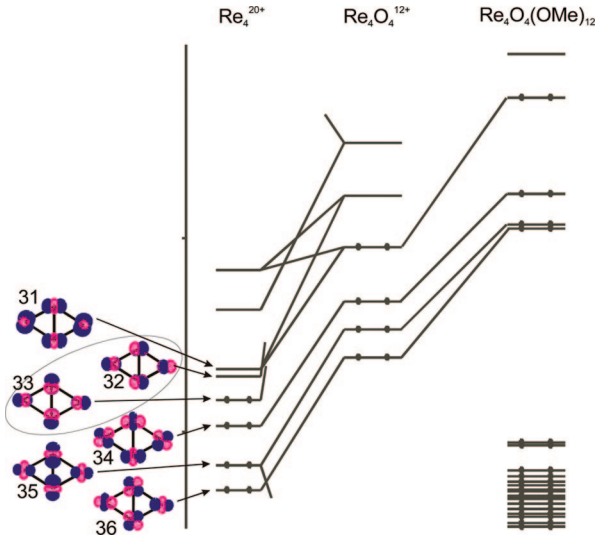

Figure 2. Molecular orbital diagram for the $Re(V)_4$ core in the ligand-free cluster in comparison with the cluster supported by oxo-ligands and the model $Re_4O_4(OMe)_{12}$ molecule .

The other two symmetrical bonds are considerably longer 2.63 Å. These values are considerably higher than even the single Re−Re bond length in $Re_2O_3(OMe)_6$ (2.56 Å[7,11]), where the metal atoms as well as those in $Re_4O_4(OEt)_{12}$ are connected by both oxo- and alkoxo-bridges. The observed difference from bonding in $Re_4O_6(O^iPr)_{10}$ can be explained by the difference in the nature of bridging ligands—introduction of two alkoxide oxygen ligands instead of the oxo-bridges results in a change in the sequence of bonding orbitals. The highlighted orbitals 32 and 33 would be most efficient in the $d_\pi-p_\pi$ interaction with oxo-ligands capping the four edges of the cluster. In the case of $Re_4O_4(OEt)_{12}$, two of the oxygen atoms from the OEt groups do not possess the necessary vacant p orbitals, which means that the most effective interaction is achieved through orbital 31, which can "bend" toward the two remaining oxo-bridges and achieve more efficient overlap, resulting in two stronger interactions. This results in a minor change in the order of bonding orbitals, but all the four orbitals originating from four Re(V) atoms with d^2 electron configurations have well-pronounced bonding character (Figure 2).

It should be mentioned that the major energy contribution to bonding is provided by the orbitals located on the oxygen atoms of the ligands, which indicates a strongly electrostatic character of interactions between the metal centers and the ligands. The difference in the chemical composition (oxo-substitution) and the oxidation states of the metal atoms should then be sought not in the stability of the metal cluster but in the geometrical characteristics of the ligands. For the methoxide Re(VI) compound, the structure contains only two oxo-bridges as each metal center can contain four alkoxide ligands in its surroundings; the ethoxide complex involves already four oxo-bridges to compensate for the possibility of putting together two metal atoms connected with four alkoxide ligands and two—with only 3 such ligands. The isopropoxide ligand size is already too big, and the structure, following the same dense packing motive as for the ethoxide, hosts two metal atoms with three alkoxide contacts and

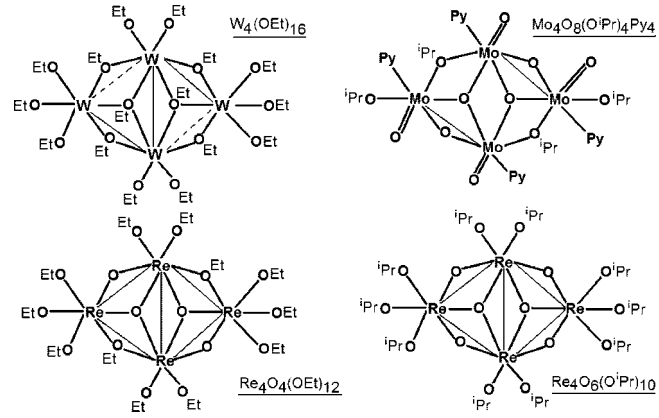

Figure 3. Schematic representation of the molecular structures with a "planar butterfly" M_4 cluster core: $W_4(OEt)_{16}$,[22] $Mo_4O_8(O^iPr)_4Py_4$,[23] $Re_4O_4(OEt)_{12}$ (this work), and $Re_4O_6(O^iPr)_{10}$.[12,17]

two—with only two alkoxides. This results in the need to incorporate six oxo-bridges in the same core. The increase in the steric tension with incorporation of a bigger alkoxide ligand can even be traced in the increase in the terminal bond lengths on the change in the radical: in the structure of $Re_4O_6(OMe)_{12}$, it is 1.883(7)−1.936(7)Å;[11] in that of the ethoxide, $Re_4O_4(OEt)_{12}$, it is 1.941(14)−2,13(2) Å; and in that of the isopropoxide, $Re_4O_6(O^iPr)_{10}$, it is 1.950(5)−2.148(6) Å.[17] The increasing donor properties of the alkyl radical do not lead thus to any shortening in the metal–oxygen bond lengths.

The same kind of core as in $Re_4O_4(OEt)_{12}$ and $Re_4O_6(O^iPr)_{10}$ with more-or-less equivalent 5 M—M distances has earlier been found exclusively in the systems with 10 cluster electrons (2 per each present M—M bond) such as, for example, in $Ba_{1.13}Mo_8O_{16}$[20] or 12 cluster electrons as in $Mo_4Br_4(O^iPr)_8$,[21] where even the elongation of terminal Mo—O bonds was observed. The withdrawal of two of the cluster electrons as in $Re_4O_4(OEt)_{12}$ compared to $Re_4O_6(O^iPr)_{10}$ leads normally to considerable elongation of two symmetrically equivalent sides of the rhombus as it was observed here and was even demonstrated earlier for such an eight-electron cluster system as $W_4(OEt)_{16}$,[22] where the longer side was found to be 2.94 Å, the shorter side being 2.65 Å, and the short diagonal being 2.76 Å. The known four-electron systems reveal only two localized metal—metal bonds, as it has been observed in $Mo_4O_8(O^iPr)_4Py_4$[23] (see Figure 3) and, more recently, in the series of complexes $PyH_2[Mo_4O_8(OMe)_2(MeOH)_2X_4]$, X = Cl, Br.[24] The present cluster represents therefore together with its close analogue $Re_4O_6(O^iPr)_{10}$, supposedly, an unusual case of conjugation of metal—metal bonds, leading to their strengthening and decreased difference in length within the cluster. It should be mentioned that the shortening of Re—Re bonds on

(20) McCarley, R. E.; Luly, M. H.; Ryan, T. R.; Torardi, C. C. *ACS Symp. Ser.* **1981**, *155*, 41.
(21) Chisholm, M. H.; Clark, D. L.; Errington, R. J.; Folting, K.; Huffman, J. C. *Inorg. Chem.* **1988**, *27*, 2071.
(22) Chisholm, M. H.; Huffman, J. C.; Kirkpatrick, C. C.; Leonelly, J.; Folting, K. *J. Am. Chem. Soc.* **1981**, *103*, 6039.
(23) Chisholm, M. H.; Folting, K.; Huffman, J. C.; Kirkpatrick, C. C. *Inorg. Chem.* **1984**, *23*, 1021.
(24) (a) Modec, B.; Brencic, J. V.; Zubieta, J. *Dalton Trans.* **2002**, 1500. (b) Modec, B.; Brencic, J. V. *Eur. J. Inorg. Chem.* **2005**, 1698.

conjugation has already been noticed earlier in the structural chemistry of Re. For example, the Re—Re distances in the $Re_3(\mu\text{-}O^iPr)_3(O^iPr)_6$ triangle, containing three Re═Re bonds, have an average of 2.36 Å,[25] compared with 2.5319(7) in $Re_2(OMe)_{10}$.[10]

Decomposition in Air and Thermal Decomposition. Crystals, taken directly from the mother solution, were gently dried on a paper and then transferred into a Pt-crucible for TG studies and an aluminum crucible for the DSC measurement setup. A fresh sample was taken to each experiment. The X-ray powder pattern taken from a fresh sample is shown in Figure S2a in the Supporting Information. A simulated X-ray powder pattern generated by ATOMS software[26] based on the parameters from the single-crystal X-ray study of $Re_4O_4(OEt)_{12}$ (−120 °C) is given in Figure S2b. The difference in peak positions and intensities indicates that $Re_4O_4(OEt)_{12}$ is not stable at ambient atmosphere. Figure S2c illustrates a theoretical X-ray powder pattern calculated of a hypothetical structure model of $Re_4O_6(OEt)_{10}$ related to that of $Re_4O_6(O^iPr)_{10}$[17] (see Figure 3). The latter pattern shows several strong peaks in the low 2θ region ($8° < 2\theta < 18°$), which are similar to those in the experimental pattern in Figure S2a. The X-ray results thus indicate that an oxidation process of $Re_4O_4(OEt)_{12}$ to $Re_4O_6(OEt)_{10}$ is in progress when $Re_4O_4(OEt)_{12}$ is exposed to ambient atmosphere. The only partial transformation in air indicates the high stability of the Re_4-cluster core. The dense packing of the molecules in the structure apparently additionally stabilizes the product. It should be mentioned that an analogous partial transformation has been described for rhenium oxomethoxide, $Re_4O_{6-x}(OMe)_{12+x}$,[11] which was also characterized by low solubility and high stability in ambient atmosphere.

Nitrogen gas was used as a protecting atmosphere against further oxidation of the rhenium oxoethoxide sample during the thermal analysis studies. The experiments were performed in the temperature range 20−450 °C (TG) and up to 600 °C (DSC), by a heating rate of 10 °C min^{-1}. The TG samples, that had been heated to 250, 300, and 450 °C, were after cooling down to room temperature taken out from the nitrogen atmosphere and stored for further X-ray powder and electron microscopy characterizations. The first sample (250 °C) reacted spontaneously with air forming a white smoke. Due to the reaction, the color of the sample changed from deep red to black. The second sample (heated up to 300 °C) was black in color and seemed to be stable in air, as no reaction could be observed, when it was transferred into the test tube. The last sample (450 °C) showed metallic color and seemed to be stable, when exposed to the air. The TG curve in Figure 4 shows a total weight loss of 44%, which corresponds well to the theoretical value of 44.8% calculated for the formation of rhenium metal from $Re_4O_6(OEt)_{10}$. This is in agreement with our results from the X-ray powder study above.

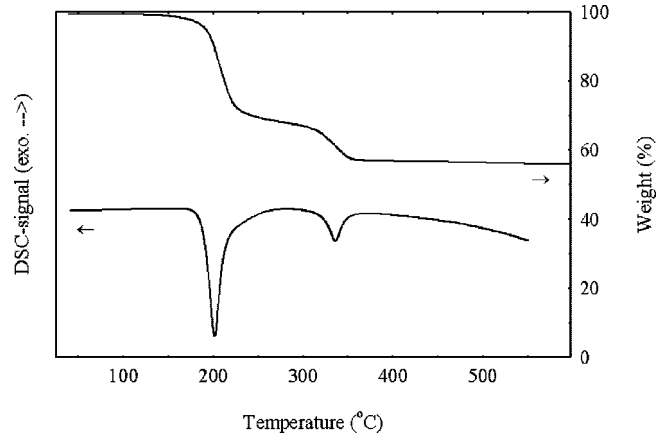

Figure 4. Thermal decomposition of fresh rhenium oxoethoxide samples in N_2 atmosphere.

After the DSC experiment, the sample exhibited a black color, probably due to interaction with residual carbon at higher temperatures, close to 600 °C. The two decomposition steps shown by TG experiment are in the DSC measurements observed as two endothermal processes, where the first step might consist of two overlapping processes or one reaction strongly controlled by diffusion processes. The first transformation of rhenium oxoethoxide started at 187.9 °C with an uptake of 2.9 kJ/g (2982.2 J/g), and the second transformation started at 321.2 °C with an uptake of 0.6 kJ/g (616 J/g (see Figure 4)). After the second decomposition step, the product had a shiny metallic color, according to the visual observations made both after TG and DSC measurements and thus indicating that Re metal particles had been formed.

The formation of Re metal was confirmed by the X-ray powder pattern of the product (see Table S1 in the Supporting Information). A peak with maximum intensity at $2\theta = 42.806°$ was in good agreement with the characteristic peak position in the X-ray diffraction pattern of the stable hexagonal modification of Re metal [ICDD-JCPDS no. 05-0702]. The observed X-ray pattern could not be associated with any Re oxide material. The metal surface might be oxidized in subsequent contact with air, however.

TEM studies of the products showed that the material at 450 °C consisted of strongly agglomerated nanocrystals. The ED pattern in Figure 5 shows a broad strong rather diffuse white ring corresponding to d values of 2.1−2.2 Å. Calculation using the line width at $2\theta = 40.3°$ and the Scherer formula for spherical crystals gave a mean crystal size of approximate 3 nm, which is also confirmed by the TEM images (see Figure 6). EDS analyses in TEM confirmed that the material consisted of Re and no other elements with atomic numbers 11 (Na) or higher.

The occurrence of deeper reduction of in the precursor compound was confirmed by the GC-MS analysis of the organic reaction byproducts. In addition to water and the parent alcohol, found normally as the major products of decomposition of the alkoxide complexes, and diethylether—the product of dealkylation without change in the oxidation state—we observed here relatively high amounts of acetaldehyde, the first oxidation product of ethanol, and even comparable with it amounts of ester—ethylacetate. The latter

(25) Hoffman, D. M.; Lappas, D.; Wierda, D. A. *J. Am. Chem. Soc.* **1993**, *115*, 10538.
(26) *ATOMS for Windows*, V6.3; Shapesoftware Inc.: Kingsport, USA, 2006.

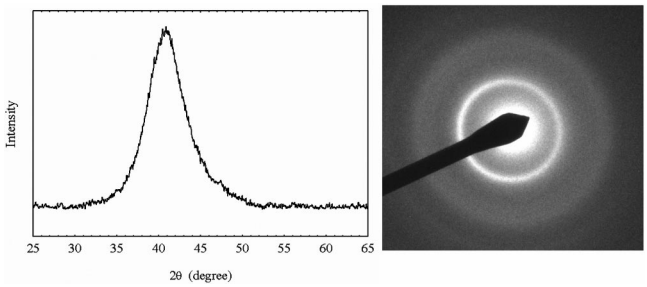

Figure 5. XRD and ED pattern of rhenium oxoethoxide heated at 450 °C in nitrogen.

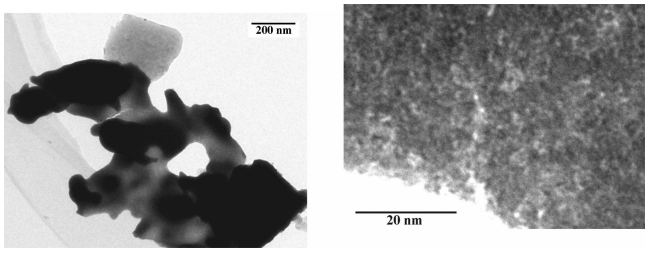

Figure 6. TEM micrographs of rhenium oxoethoxide heated at 450 °C, in nitrogen.

results from two-electron oxidation of the alkoxide ligands. It has thus been envisaged that the thermal decomposition of $Re_4O_4(OEt)_{12}$ occurs in a principally different way than that for oxomethoxide, $Re_4O_6(OMe)_{12}$, and for isopropoxide, $Re_4O_6(O^iPr)_{10}$, where trace amounts or no related esters could be observed, ReO_3 being the only product of the first step in decomposition, which resulted finally in ReO_2 stable to at least 800 °C (see the reaction scheme below).

$$Re_4O_6(OMe)_{12} \rightarrow ReO_3 + H_2O + MeOH + Me_2O + CH(OMe)_2 + \text{traces } HCOOMe$$

$$Re_4O_4(OEt)_{12} + \text{air} \rightarrow Re_4O_6(OEt)_{10} \rightarrow Re + H_2O + EtOH + Et_2O + CH_3CHO + CH_3CHOOEt$$

Rhenium metal could be obtained from these two latter precursors only using hydrogen gas as the reductive agent. Selective and quantitative formation of rhenium metal at such a low temperature as 380 °C without introduction of any additional reductive agent makes rhenium ethoxide an attractive precursor of rhenium nanopowders highly requested by the industries for powder metallurgy applications.

Acknowledgment. The authors are indebted to the Swedish Research Council, Swedish Royal Academy of Sciences, and Russian Foundation for Basic Research for the financial support of this work. We express also our gratitude to Suresh Gohil for the assistance in the GC-MS experiments.

Supporting Information Available: Figures S1 and S2 and Table S1. This material is available free of charge via the Internet at http://pubs.acs.org. Crystallographic data for the structural analysis have been deposited with the Cambridge Crystallographic Data Centre. Copies of this information can be obtained free of charge via www.ccdc.cam.ac.uk/conts/retrieving.html (or from the Cambridge Crystallographic Data Centre, 12 Union Road, Cambridge CB2 1EZ, UK. Fax: +44-1223-336033. E-mail: deposit@ccdc.cam.ac.uk).

IC701781K